

Instability of Massive Scalar Fields in Kerr-Newman Spacetime

Hironobu FURUHASHI^{*)} and Yasusada NAMBU^{**)}

*Department of Physics, Graduate School of Science, Nagoya University,
Chikusa, Nagoya 464-8602, Japan*

Abstract

We investigate the instability of charged massive scalar fields in Kerr-Newman spacetime. Due to the super-radiant effect of the background geometry, the bound state of the scalar field is unstable, and its amplitude grows in time. By solving the Klein-Gordon equation of the scalar field as an eigenvalue problem, we numerically obtain the growth rate of the amplitude of the scalar field. Although the dependence of the scalar field mass and the scalar field charge on this growth rate agrees with the result of the analytic approximation, the maximum value of the growth rate is three times larger than that of the analytic approximation. We also discuss the effect of the electric charge on the instability of the scalar field.

^{*)} E-mail: hironobu@gravity.phys.nagoya-u.ac.jp

^{**)} E-mail: nambu@gravity.phys.nagoya-u.ac.jp

§1. INTRODUCTION

The propagation of waves in black hole spacetime has been studied by many researchers in the context of black hole perturbations.¹⁾ Super radiance is one type of interesting phenomena related to this topic.^{2),3),4),5)} Considering the situation that a wave impinges on a black hole, the incident wave is partially reflected by the potential barrier of the black hole, due to the centrifugal force, and is scattered to infinity, while part of the wave penetrates the potential barrier and is absorbed by the black hole. Thus, one would expect that the amplitude of the scattered waves is always smaller than that of the incident wave. However, this is not necessarily true in the Kerr-Newman geometry. If the frequency of the incident wave satisfies the so-called super-radiant condition, the reflected wave is amplified, and its amplitude becomes larger than that of the incident wave; that is, the reflection rate can be greater than unity. Using this amplification mechanism, it is possible to extract the rotation and the electro-static energy of Kerr-Newman black holes.

As an application of the super radiance, Press and Teukolsky proposed the “black hole bomb”.⁶⁾ They considered the situation in which mirrors surround a Kerr black hole. Then, the scattered wave with super-radiant amplification is reflected back to the black hole by the mirrors, and the wave is amplified again. In this way, the amplitude of the wave grows exponentially in time and becomes unstable. Damour *et al.*⁷⁾ have shown that a black hole bomb can be realized by using a charged massive scalar field in Kerr-Newman spacetime. The effective potential of the massive scalar field has a local minimum, and the scalar field wave can be confined in this potential well. Hence, the mass of the scalar field plays the role of the mirrors, which is necessary to cause the instability of the scalar field. According to their analysis, the instability of the scalar field is realized if the bound state and the super-radiant condition are both satisfied.

To evaluate the growth rate of the scalar field, we must solve the Klein-Gordon equation in the black hole geometry. By imposing ingoing boundary conditions at the black hole horizon and regular boundary conditions at infinity, the problem of obtaining the unstable mode reduces to an eigenvalue problem. For Kerr spacetime, the growth rate of the unstable modes for a scalar field with a small mass $\mu \ll 1/M$ (where M is the mass of the black hole) was obtained by using the asymptotic matching method,⁸⁾ and that for a large mass $\mu \gg 1/M$ was obtained by using the WKB approximation.⁹⁾ However, these analyses do not cover the parameter region in which $\mu M \sim 1$, where the growth rate is expected to take its maximum value.

In this paper, we aim to obtain the growth rate of a charged massive scalar field with mass satisfying $\mu M \lesssim 1$ in Kerr-Newman spacetime by solving the eigenvalue problem

numerically. The paper is organized as follows. In §2, we estimate the growth rate of a scalar field with $\mu M \ll 1$ and $qQ \ll 1$ in Kerr-Newman spacetime using the method of Detweiler.⁸⁾ Then, in §3, we introduce our numerical method and obtain the growth rate caused by the instability and its parameter dependence for $\mu M \lesssim 1$. Section 4 is devoted to a summary and conclusion.

We use the units in which $G = c = \hbar = 1$ throughout the paper.

§2. Analytic approach

In this section, we calculate the growth rate of the scalar field using the asymptotic matching method used by Detweiler⁸⁾ in Kerr-Newman spacetime.

The Kerr-Newman metric in the Boyer-Lindquist coordinates is

$$\begin{aligned}
 ds^2 = & - \left(1 - \frac{2Mr - Q^2}{\Sigma} \right) dt^2 - \frac{(2Mr - Q^2)2a \sin^2 \theta}{\Sigma} dt d\phi \\
 & + \frac{\Sigma}{\Delta} dr^2 + \Sigma d\theta^2 + \left(r^2 + a^2 + \frac{(2Mr - Q^2)a^2 \sin^2 \theta}{\Sigma} \right) \sin^2 \theta d\phi^2, \\
 \Delta = & r^2 - 2Mr + a^2 + Q^2, \quad \Sigma = r^2 + a^2 \cos^2 \theta,
 \end{aligned} \tag{1}$$

where M is the mass, a is the angular momentum and Q is the electric charge of the black hole. The locations of the horizons r_{\pm} are given by the roots of the equation $\Delta = 0$. The Klein-Gordon equation for a charged scalar field with mass μ is

$$\begin{aligned}
 (\nabla^\alpha - iqA^\alpha)(\nabla_\alpha - iqA_\alpha)\Psi &= \mu^2\Psi, \\
 A_\alpha &= \left(-\frac{rQ}{\Sigma}, 0, 0, \frac{aQr}{\Sigma} \sin^2 \theta \right),
 \end{aligned} \tag{2}$$

where ∇^α is the covariant derivative in the Kerr-Newman geometry, and q is the charge of the scalar field. Equation (2) is separable in terms of the spheroidal harmonics $S(\theta)$:

$$\Psi = \psi(r)S(\theta) \exp(i(-\omega t + m\phi)). \tag{3}$$

The radial function $\psi(r)$ satisfies the relation

$$\Delta \frac{d}{dr} \Delta \frac{d\psi}{dr} + \left[-\Delta(\mu^2 r^2 + \lambda) + \{(r^2 + a^2)\omega - ma - qQr\}^2 \right] \psi = 0, \tag{4}$$

with

$$\lambda = l(l+1) - 2maw + (a\omega)^2 + O(a^2\mu^2(1 - \omega^2/\mu^2)),$$

where l, m are integers and $|m| \leq l$. We assume $l \geq 1$. (For $l = 0$, there is no centrifugal force, and the bound state of the scalar field does not exist.) We are interested in the eigenmode whose frequency is nearly equal to the mass of the scalar field, i.e. for which $\omega \sim \mu$. As in this case we have $|1 - \omega^2/\mu^2| \ll 1$, we can realize the relation $O(a^2\mu^2(1 - \omega^2/\mu^2)) \sim 0$, and then the separation constant is given by

$$\lambda = l(l+1) - 2ma\omega + (a\omega)^2. \quad (5)$$

We solve Eq.(4) using regular boundary conditions at infinity and ingoing boundary conditions at the black hole horizon. To apply the asymptotic matching method, we need to assume that the parameters satisfy the conditions

$$O(|\omega M|) = O(\mu M) = O(qQ) \equiv O(\epsilon), \quad \epsilon \ll 1, \quad (6)$$

and that they can thus be treated as small parameters. The angular momentum of the black hole is assumed to satisfy $O(a/M) = 1$.

For large r , i.e. $r \gg r_+$, Eq. (4) reduces to

$$\frac{d^2}{dr^2}(\Delta^{1/2}\psi) + \left[\omega^2 - \mu^2 + \frac{2(2M\omega^2 - M\mu^2 - qQ\omega)}{r} - \frac{l(l+1) + \epsilon^2}{r^2} \right] (\Delta^{1/2}\psi) = 0. \quad (7)$$

To satisfy the regular boundary conditions at infinity, the phase of ω is required to satisfy

$$0 < \arg \sqrt{\omega^2 - \mu^2} < \pi. \quad (8)$$

The solution of this equation that is regular at infinity is

$$\begin{aligned} r\psi &= (-2ikr)^{l+1} e^{ikr} U(l+1 - \nu + \epsilon^2, 2l+2 + 2\epsilon^2, -2ikr), \\ k &= \sqrt{\omega^2 - \mu^2}, \quad \nu = \frac{2M\omega^2 - M\mu^2 - qQ\omega}{-ik}, \end{aligned} \quad (9)$$

where U is one of the confluent hypergeometric functions.¹⁰⁾ The asymptotic behavior of the solution (9) for $|kr| \ll 1$ takes the form

$$\begin{aligned} r\psi &\sim \frac{(-2ikr)^{l+1} \pi}{\sin[\pi(2l+2+2\epsilon^2)]} \\ &\times \left\{ \frac{1}{\Gamma(-l-\nu-\epsilon^2)\Gamma(2l+2+2\epsilon^2)} + \cdots \right. \\ &\quad \left. - (-2ikr)^{-2l-1} \frac{1}{\Gamma(l-\nu+1+\epsilon^2)\Gamma(-2l-2\epsilon^2)} + \cdots \right\}. \end{aligned} \quad (10)$$

In the region near the black hole horizon ($r \ll l/\mu$), Eq. (4) reduces to

$$z \frac{d}{dz} z \frac{d}{dz} \psi + \left[P^2 - l(l+1) \frac{z}{(1-z)^2} \right] \psi = 0, \quad (11)$$

$$z = \frac{r - r_+}{r - r_-}, \quad P = -\frac{(r_+^2 + a^2)\omega - ma - qQr_+}{r_+ - r_-},$$

and the solution with ingoing boundary conditions at the horizon is given by

$$\psi = z^{iP} (1-z)^{l+1} F(l+1, l+1+2iP, 1+2iP, z), \quad (12)$$

where F is the Gauss hypergeometric function. The asymptotic form of the solution (12) for $1-z \ll 1$ is given by

$$\begin{aligned} \psi \sim & \frac{\Gamma(1+2iP)\Gamma(2l+1)}{\Gamma(l+1)\Gamma(l+1+2iP)} \left(\frac{r}{r_+ - r_-} \right)^l + \dots \\ & + \frac{\Gamma(1+2iP)\Gamma(-2l-1)}{\Gamma(-l)\Gamma(-l+2iP)} \left(\frac{r}{r_+ - r_-} \right)^{-l-1} + \dots \end{aligned} \quad (13)$$

We get the asymptotic behavior described by (10) and (13). These expressions are valid in the ranges $r_+ \ll r \ll 1/k$ and $r_+ \ll r \ll l/\mu$, respectively. Consequently, for $\omega \sim \mu$, we have the overlap region in which both the outer expansion (10) and the inner expansion (13) hold:

$$r_+ \ll r \ll \frac{1}{2\sqrt{\mu^2 - \omega^2}}. \quad (14)$$

In this region, we can match the leading-order terms of the solutions (10) and (13), and this matching yields

$$\frac{\Gamma(-l - \nu - \epsilon^2)\Gamma(2l+2)}{\Gamma(l - \nu + 1 + \epsilon^2)\Gamma(-2l - 2\epsilon^2)} = -2P [2k(r_+ - r_-)]^{2l+1} \prod_{j=1}^l (j^2 + 4P^2) \frac{\Gamma(l+1)\Gamma(-2l-1)}{\Gamma(2l+1)\Gamma(-l)}. \quad (15)$$

For $\omega \sim \mu$ and $k(r_+ - r_-) \ll 1$, the right-hand side of the this equation is $O((k(r_+ - r_-))^{2l+1})$. Therefore, we define $\nu^{(0)}$ as the value of ν for which the right-hand side equals zero and write $\nu \equiv \nu^{(0)} + \delta\nu$.

For $\nu = \nu^{(0)}$, the matching condition (15) yields

$$\frac{\Gamma(-l - \nu^{(0)} - \epsilon^2)\Gamma(2l+2)}{\Gamma(l - \nu^{(0)} + 1 + \epsilon^2)\Gamma(-2l - 2\epsilon^2)} = 0. \quad (16)$$

Thus, using the property of the gamma function $1/\Gamma(-n) = 0$, we have

$$l - \nu^{(0)} + 1 + \epsilon^2 = -n, \quad (17)$$

where $n = 0, 1, 2, \dots$. From the definition of ν and Eq. (9), we find

$$\nu^{(0)} = \frac{2M\omega^{(0)2} - M\mu^2 - qQ\omega^{(0)}}{-i\sqrt{\omega^{(0)2} - \mu^2}} \simeq l + n + 1, \quad (18)$$

$$\omega^{(0)} \simeq \mu \left[1 - \left(\frac{M\mu - qQ}{l + n + 1} \right)^2 \right]^{1/2} \simeq \mu \left[1 - \frac{1}{2} \left(\frac{M\mu - qQ}{l + n + 1} \right)^2 \right], \quad (19)$$

$$k^{(0)} = \sqrt{\omega^{(0)2} - \mu^2} \simeq i \frac{M\mu - qQ}{l + n + 1} \mu. \quad (20)$$

From Eqs. (8) and (20), to satisfy the regular boundary conditions at infinity, we must require the condition

$$M\mu \gtrsim qQ. \quad (21)$$

With this condition, the effective potential has a well (see Fig. 2), and this condition guarantees that the wave is confined in this well.

Next, we obtain $\delta\nu$ perturbatively. The left-hand side of Eq. (15) becomes

$$\frac{\Gamma(-l - \nu^{(0)} - \epsilon^2)\Gamma(2l + 2)}{\Gamma(l - \nu^{(0)} + 1 + \epsilon^2)\Gamma(-2l - 2\epsilon^2)} [1 + \{\psi(l - \nu^{(0)} + \epsilon^2) - \psi(-l - \nu^{(0)} - \epsilon^2)\}\delta\nu], \quad (22)$$

with

$$\psi(z) = \Gamma'(z)/\Gamma(z).$$

Then, using the property of the gamma function

$$\lim_{z \rightarrow -n} \frac{\psi(z)}{\Gamma(z)} = (-1)^{n+1} n!, \quad \frac{\Gamma(-n)}{\Gamma(-m)} = \frac{(-1)^{n-m} m!}{n!}, \quad (23)$$

we find $\delta\nu$ as

$$\delta\nu = 2iP^{(0)} \left[\frac{2(M\mu - qQ)}{l + n + 1} \mu(r_+ - r_-) \right]^{2l+1} \times \frac{(2l + n + 1)!}{n!} \left[\frac{l!}{(2l)!(2l + 1)!} \right]^2 \prod_{j=1}^l (j^2 + 4P^{(0)2}), \quad (24)$$

where

$$P^{(0)} = -\frac{(r_+^2 + a^2)\omega^{(0)} - ma - qQr_+}{r_+ - r_-}.$$

Here, the relation between $\delta\nu$ and $\delta\omega$ is given by

$$\delta\nu = \mu \frac{M\mu - qQ}{i} \frac{\omega^{(0)}\delta\omega}{k^{(0)3}} = \frac{(l + n + 1)^3}{(M\mu - qQ)^2} \frac{\delta\omega}{\mu}. \quad (25)$$

Thus, the real part σ and the imaginary part γ of the leading-order contribution to the eigenvalue ω are

$$\sigma = \mu \left[1 - \frac{1}{2} \left(\frac{M\mu - qQ}{l+1+n} \right)^2 \right] = \mu [1 - O(\epsilon^2)], \quad (26)$$

$$\gamma = \mu \frac{\delta\nu}{i} \frac{(M\mu - qQ)^2}{(l+1+n)^3} = O(\epsilon^{4l+5}). \quad (27)$$

If the imaginary part γ of ω is positive, the mode in question is unstable, and γ represents the growth rate of the scalar field. From Eqs. (24) and (27), the condition for the existence of an instability is

$$P^{(0)} = \frac{1}{2\kappa} (m\Omega^H + q\Phi^H - \sigma) > 0, \quad (28)$$

where the surface gravity κ , the angular velocity Ω^H , and the electric potential Φ^H for the Kerr-Newman black hole are introduced as follows:

$$\kappa = \frac{1}{2} \left(\frac{r_+ - r_-}{a^2 + r_+^2} \right), \quad \Omega^H = \frac{a}{a^2 + r_+^2}, \quad \Phi^H = \frac{Qr_+}{a^2 + r_+^2}. \quad (29)$$

The condition of instability (28) coincides with that of super-radiance. If the super-radiant condition is compatible with the condition for the existence of bound state (21), the scalar field becomes unstable. These features of the unstable mode are consistent with the results of the analysis carried out by Damour *et al.*⁷⁾ The most unstable mode corresponds to $l = m = 1$ and $n = 0$, and the value of γ for this mode is given by

$$\gamma = \frac{\mu^4}{24} |M\mu - qQ|^5 (a^2 + r_+^2)^3 (\Omega^H + q\Phi^H - \mu) (\kappa^2 + (\Omega^H + q\Phi^H - \mu)^2). \quad (30)$$

For the extreme case in which $a^2 + Q^2 = M^2$, γ becomes

$$\gamma = \frac{\mu^4}{24} (a^2 + M^2)^3 |M\mu - qQ|^5 (\Omega^H + q\Phi^H - \mu)^3. \quad (31)$$

For a Kerr black hole ($Q = 0$), γ reduces to

$$\gamma M = \frac{a}{M} \frac{(\mu M)^9}{24}, \quad (32)$$

which is the formula derived by Detweiler.⁸⁾

The mass and charge dependences of γ are displayed in Fig. 1. The maximum value is $\gamma \approx 3 \times 10^{-8}$, realized at $\mu M \approx 0.3$, $qQ \approx -0.08$. The value of γ is positive in the region where both the super-radiant condition $P^{(0)} > 0$ and the bound state condition $M\mu \gtrsim qQ$ are satisfied. Let us consider the region satisfying $\mu M \ll 1$, $|qQ| \ll 1$, where our approximation

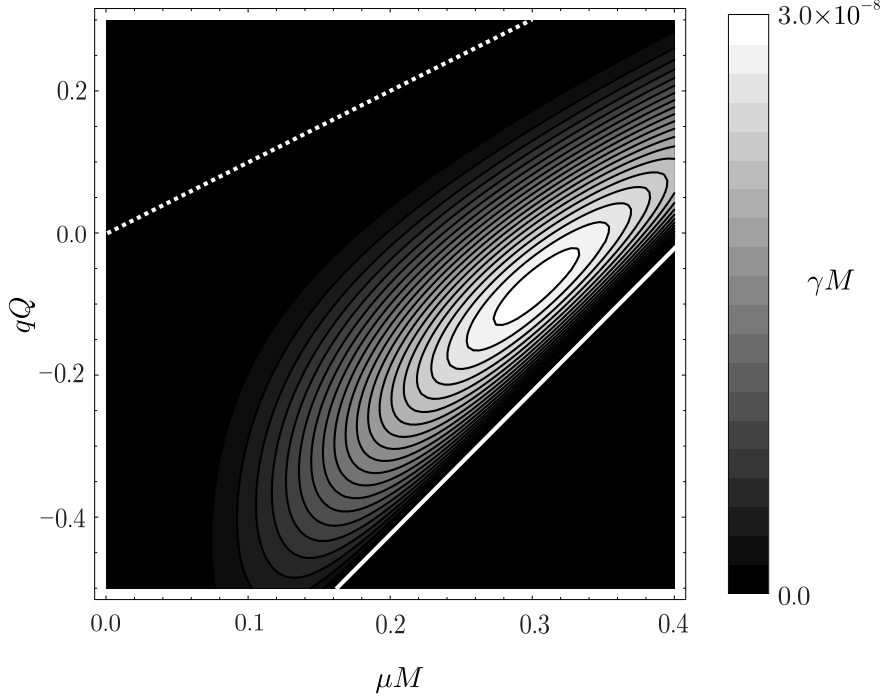


Fig. 1. The dependence of the mass μ and the charge q of the scalar field on the growth rate γ . The parameter values here are $a = 0.98M$, $Q = 0.01M$, $l = m = 1$, and $n = 0$. The solid line corresponds to $P^{(0)} = 0$, and the dotted line corresponds to $M\mu - qQ = 0$.

is expected to be good. In this region, retaining only the leading-order terms of the small parameters, γ becomes

$$\gamma \approx \frac{\mu^4}{24} |M\mu - qQ|^5 a (M^2 - Q^2) \quad (33)$$

and the (μ, q) dependence of γ is determined by the factor $\mu^4 |M\mu - qQ|^5$. For a fixed value of q , γ is an increasing function of μ , for a fixed value of μ , γ is a decreasing function of qQ . Equation (33) shows that the main effect of the scalar field charge q is to change the depth of the potential well that is necessary to bound the scalar field. As the charge q increases, the depth of the well of the scalar field effective potential decreases, and the scalar field becomes less bounded. Thus, an increase of the charge decreases the growth rate of the scalar field.

For a positive charge, i.e. $q > 0$, $P^{(0)}$ can be positive for a negative azimuthal quantum number $m < 0$. This contrasts with the case of a Kerr black hole, which requires $m > 0$ to realize $P^{(0)} > 0$. This indicates the possibility of an unstable mode with $m < 0$. For $m < 0$, the condition $P^{(0)} > 0$ is

$$-|m\Omega^H| M - \left(1 - \frac{r_+ M}{a^2 + r_+^2}\right) qQ > \mu M - qQ \quad (34)$$

for $qQ > 0$. However, the left-hand side of this inequality is negative, and thus Eq. (34) cannot be compatible with the bound state condition (21). Thus for $q > 0$ and $m \leq 0$ in

Kerr-Newman spacetime, super radiance occurs, but the scalar field cannot be in a bound state, and the mode is stable. For Reissner-Nordström spacetime we have $a = 0$, and the relation $P^{(0)} > 0$ gives

$$\mu < \frac{qQ}{r_+}. \quad (35)$$

This condition also cannot be compatible with the bound state condition (21), and we conclude that there is no unstable mode of the scalar field in Reissner-Nordström spacetime. From these results, it is seen that the super radiance caused by the rotation of the black hole is essential to make the scalar field unstable.

§3. Numerical approach

3.1. Method

To investigate the instability of the scalar field for a wide range of parameter values, we carried out numerical calculations. For this purpose, we first rewrite Eq. (4) in terms of the tortoise coordinate

$$x = \int dr \frac{r^2}{\Delta} = r + \frac{1}{r_+ - r_-} [r_+^2 \ln(r - r_+) - r_-^2 \ln(r - r_-)] \quad (36)$$

and the new radial function $u = r\psi$. We then obtain

$$\begin{aligned} \frac{d^2 u}{dx^2} &= V_{\text{eff}}(r)u, \\ V_{\text{eff}}(r) &= \frac{\Delta}{r^2} \left[\mu^2 + \frac{\lambda}{r^2} + \frac{2M}{r^3} - \frac{2(a^2 + Q^2)}{r^4} \right] - \frac{1}{r^4} [(r^2 + a^2)\omega - am - qQr]^2, \\ \lambda &= l(l+1) - 2ma\omega + (a\omega)^2. \end{aligned} \quad (37)$$

The effective potential V_{eff} for $a = 0.98M$, $Q = 0.01M$, $\mu M = 0.35$, $qQ = -0.08$, $l = m = 1$ is plotted in Fig.2. Due to the mass of the scalar field, the effective potential has a well, and the wave can be trapped in this well.

In the region near the horizon, the incoming solution of Eq. (37) is given by

$$u \sim \exp \left[-i \left(\frac{2M\omega - qQ}{r_+} - \frac{am + Q^2\omega}{r_+^2} \right) x \right], \quad (38)$$

and in the far region, the regular solution of Eq. (37) is given by

$$u \sim x^{(M\mu^2 - qQ\omega)/\sqrt{\mu^2 - \omega^2}} \exp \left(-x\sqrt{\mu^2 - \omega^2} \right). \quad (39)$$

We use the solutions (38) and (39) to impose the boundary conditions for the numerical integration of Eq. (37). We prepare the inner numerical boundary $x = x_1$ near the horizon

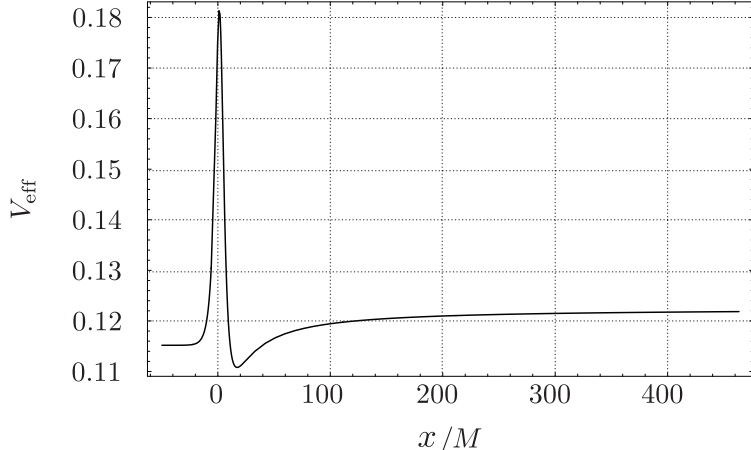


Fig. 2. The effective potential $V_{\text{eff}}(x)$ of the scalar field for $a = 0.98M$, $Q = 0.01M$, $\mu M = 0.35$, $qQ = -0.08$, $l = m = 1$.

r_+ and the outer numerical boundary $x = x_2$. By integrating Eq. (37) from $x = x_1$ with the boundary conditions given by Eq. (38), we obtain a mode function $u^{(1)}$. In the same way, we obtain $u^{(2)}$ with the boundary conditions imposed at the far region $x = x_2$. For a given complex value of ω , if the Wronskian

$$W(u^{(1)}, u^{(2)}) = u^{(1)} \frac{du^{(2)}}{dx} - u^{(2)} \frac{du^{(1)}}{dx} \quad (40)$$

evaluated at the midpoint $x = x_m (x_1 < x_m < x_2)$ is zero, the two solutions $u^{(1)}$ and $u^{(2)}$ are linearly dependent, and ω is an eigenvalue of the equation under consideration. We search for the zero point of the complex function $W(\omega)$ numerically in the complex ω plane.

3.2. Result

We performed numerical calculations to search for the mode of the scalar field satisfying $l = m = 1$ and $\omega \sim \mu$, for which the growth rate of the unstable mode is expected to have the largest value. We chose the parameter values of the black hole as $a = 0.98M$ and $Q = 0.01M$ and used the fourth-order Runge-Kutta integrator. The numerical boundaries were set at $x_1 = -50M$, $x_2 = 1510M$, $x_m = 24.5M$, and the grid spacing was $\Delta x = 0.5M$. We obtained the value of the growth rate γ as a function of the scalar field mass μ and the scalar field charge q . We calculated the values of ω for the eigenmode using 77 different sets of parameter values in (μ, q) -space. These points in (μ, q) -space are indicated in Fig.3.

For the obtained value of ω , we checked the validity of the assumption $\omega \sim \mu$ used in Eq. (37). In Fig.4, we plot $|\mu^2/\omega^2 - 1|$ as a function of μ for $q = 0$. For the obtained value of ω , this value is smaller than 5.5×10^{-2} , and our assumption $\omega \sim \mu$ and (5) are correct for the numerically obtained modes. For $q \neq 0$, this value does not exceed 10^{-2} . We also

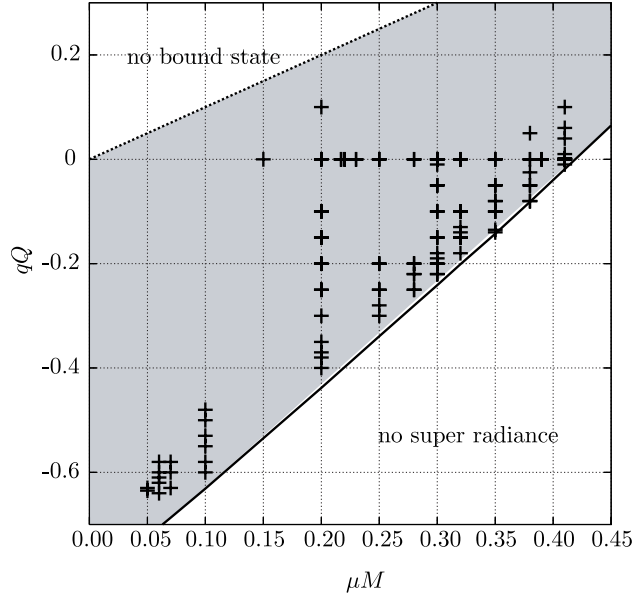


Fig. 3. The sets of parameter values used in the numerical calculations plotted corresponds to in (μ, q) -space. The solid line corresponds to $P^{(0)} = 0$ and the dotted line to $M\mu - qQ = 0$. The scalar field is expected to be unstable for sets of parameter values in the grey region.

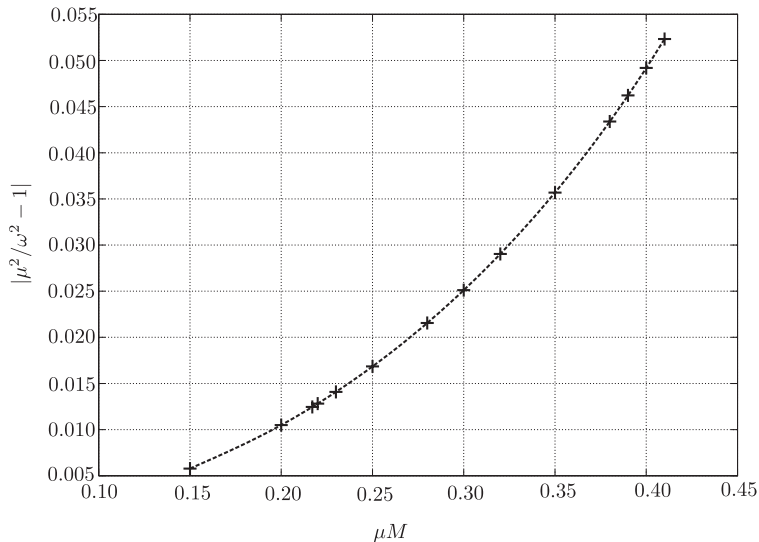


Fig. 4. The value of $|\mu^2/\omega^2 - 1|$ as a function of μ for $q = 0$. This value is less than 5.5×10^{-2} for all values of μM , and we find that our numerical results are consistent with the assumption $\omega \sim \mu$.

calculated the eigen-modes using a different grid size. To check the numerical error on the obtained value of ω , a numerical integration with $x_2 = 3000M$ was also carried out. The relative error on the value of ω evaluated from these calculations was found to be less than 10^{-3} .

The obtained growth rate is plotted in Fig. 5. It is seen that the shape of the numerically

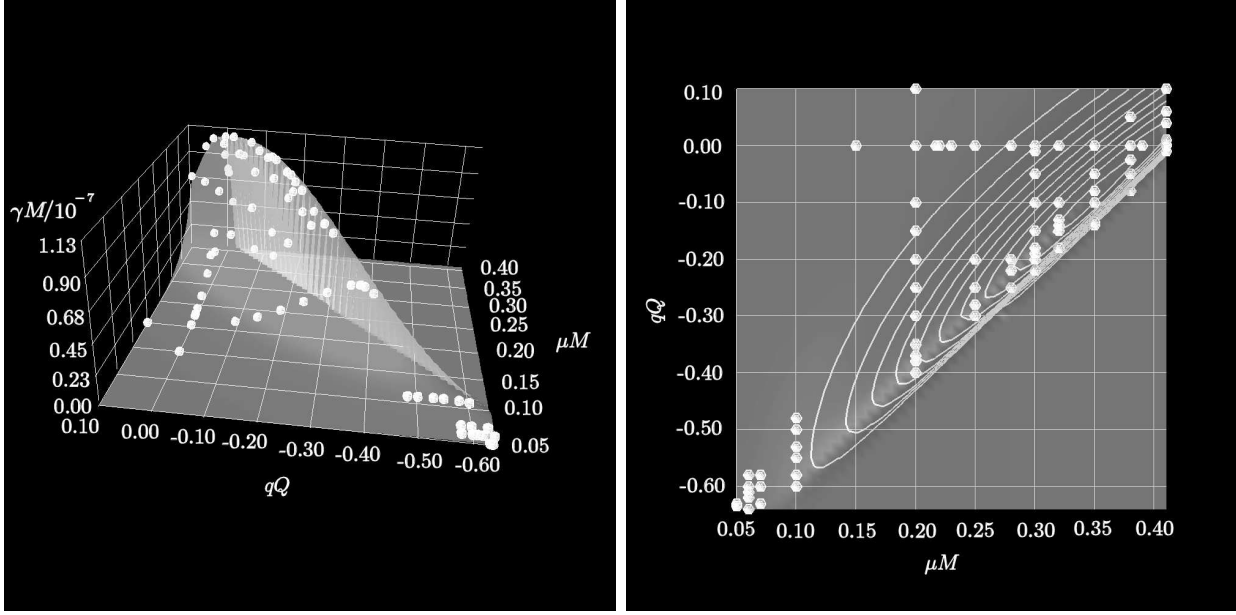


Fig. 5. The numerically obtained value of the growth rate γ . The spheres represent the obtained values of γ . The left panel is a birds-eye view of $\gamma(\mu, q)$ for $a = 0.98M$, $Q = 0.01M$, $l = m = 1$. The right panel is the same function as viewed from above.

obtained function $\gamma(\mu, q)$ is almost the same as that of the analytically obtained one (see Fig. 1). The left panel in Fig. 6 displays the μ dependence of γ for different values of q . The plus symbols represent the maximum values of γ for each μ , and the cross symbols represent γ for $q = 0$. The solid curve represents the values of γ for $q = 0$ predicted using the analytic approximation. In the region satisfying $\mu M \lesssim 0.25$, the value of the numerically obtained γ

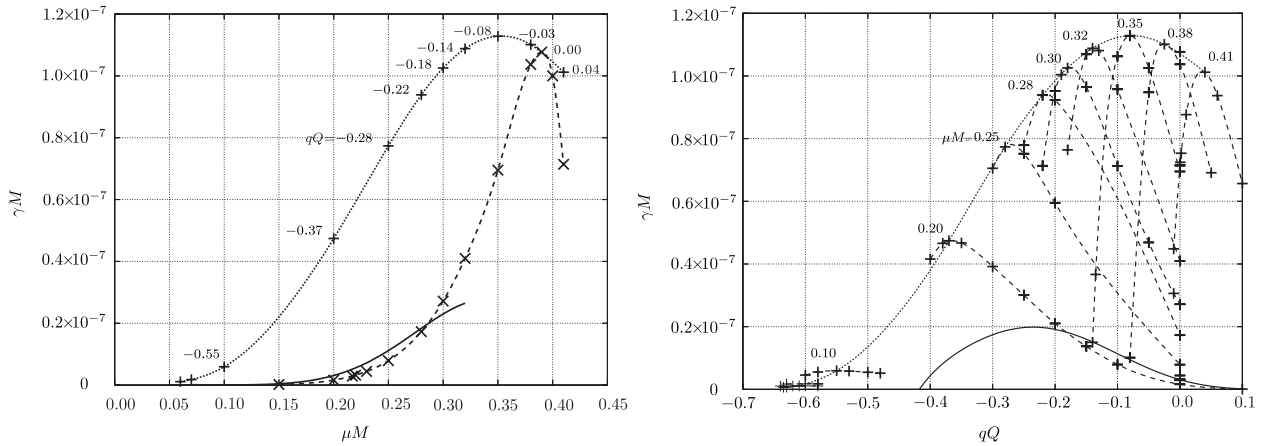


Fig. 6. The left panel displays the μ dependence of the growth rate γ for several values of q . The dashed curve represents the numerical solution for $q = 0$, and the solid curve represents the analytic approximation (30) for $q = 0$. The right panel plots the q dependence of the growth rate γ for several values of μ . The dashed curves represent γ for $\mu = 0.1 - 0.41$. The solid curve represents the analytic approximation for $\mu M = 0.20$.

approaches that of the analytic solution. The deviation from the analytic solution becomes significant for $0.3 \lesssim \mu M$. For parameter values in this region, the asymptotic matching method does not provide a good approximation. The right panel in Fig. 6 displays the q dependence of γ . The solid curve represents γ obtained using the analytic approximation for $\mu M = 0.2$, and it is seen that the approximation is good for $-0.2 \lesssim qQ$.

The growth rate has a maximum value $\gamma M \simeq 1.13 \times 10^{-7}$ at $\mu M \simeq 0.35$, $qQ \simeq -0.08$. The obtained minimum value of the growth rate is 7.6×10^{-11} at $\mu M = 0.20$, $qQ = 0.1$. Although the shape of the function $\gamma(\mu, q)$ agrees with the analytically obtained result displayed in Fig. 1, its maximum value is three times larger. We confirm that the instability exists in the region of (μ, q) -space where both the super-radiant condition $P^{(0)} > 0$ and the bound state condition $M\mu \gtrsim qQ$ are satisfied. This parameter region is also shown in Fig. 3. For all numerically obtained modes, the growth rates are positive, and they are contained in the region bounded by the two lines $P^{(0)} = 0$ and $M\mu - qQ = 0$. As the parameter point (μ, q) approaches these lines, the growth rate decreases. We conclude that, the function $\gamma(\mu, q)$ has a maximum value in this region. We could not obtain a stable mode with negative γ ; because the value of γ for the stable mode is small compared to that for the unstable mode, it was not possible to obtain a definite value within the accuracy of our numerical calculation.

In Fig. 7, we show the behavior of the mode functions for the stable and unstable cases. The mode function of the stable mode $m = -1$ increases monotonically while moving toward

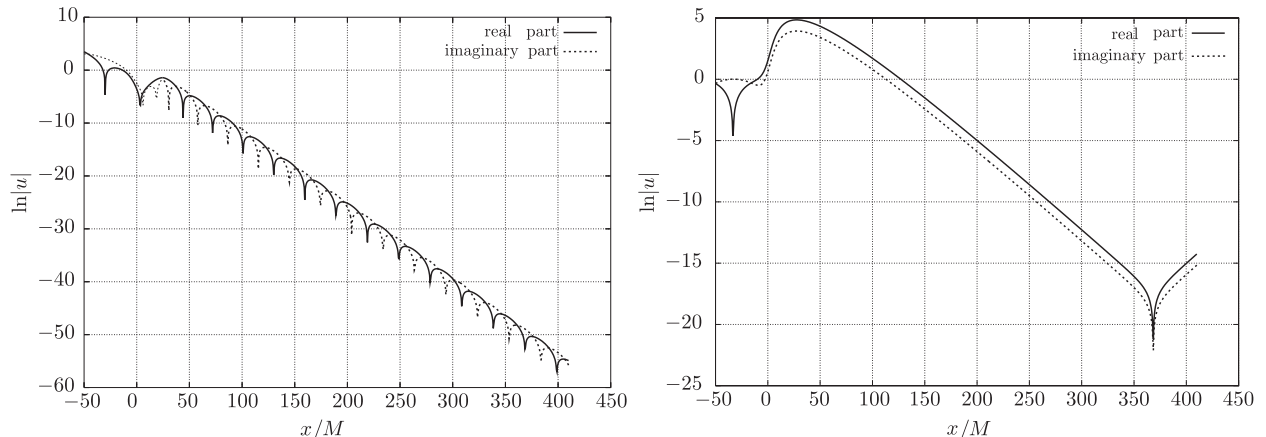


Fig. 7. The behavior of the mode functions $u(x)$. The solid curve is the real part and the dotted curve is the imaginary part of $u(x)$. The left panel plots the mode function of the stable mode $m = -1$. The right panel plots the mode function of the unstable mode $m = 1$. The parameter values are $a = 0.98M$, $Q = 0.01M$, $\mu M = 0.35$, $qQ = -0.08$, $l = 1$.

the horizon of the black hole. Contrastingly, the mode function of the unstable mode $m = 1$ has a maximum at $x \simeq 27.5M$. This location corresponds to the minimum of the effective potential (see Fig. 2). For both values $m = \pm 1$, the effective potential has a well, which is

necessary in order for a bound state to exist. However, for the $m = -1$ mode, the super-radiant condition is not satisfied, and the wave falls into the black hole through the potential barrier. For the $m = 1$ mode, the super-radiant effect is significant, and the amplified wave can accumulate in the potential well. This leads to the instability of the mode.

§4. Summary and discussion

In this paper, we have studied the unstable modes of a massive scalar field in Kerr-Newman spacetime. We obtained the leading-order value of the growth rate for $\mu M \ll 1$, $qQ \ll 1$ using the asymptotic matching method and for $\mu M \lesssim 1$ using a numerical method. For a black hole with $a = 0.98M$, $Q = 0.01M$, we obtained the maximum value of the growth rate of the unstable mode to be $\gamma M \simeq 1.13 \times 10^{-7}$ for $\mu M \simeq 0.35$, $qQ \simeq -0.08$. The location of the maximum value in (μ, q) -space agrees with the result of the analytic method, but its numerical value is three times larger than that of the analytic result. For $0.3 \lesssim \mu M$, the numerically obtained value of γ deviates significantly from that of the analytic result. This indicates that the asymptotic matching method does not give a good approximation in this parameter region. If the mass of the scalar field is $\mu \gg 1$ [MeV], the mass of the black hole must be $M \ll 10^{15}$ [Kg] for that the instability to be maximal. Thus, there is a possibility that the mechanism of the black hole bomb can influence the evolution of primordial black holes.

To investigate the dynamics of the unstable mode, it is interesting to consider the temporal evolution of a scalar wave with an unstable mode in the black hole geometry. The propagation of such a wave in black hole spacetime consists of three stages. During the first stage, there is a burst wave that depends on the initial conditions of the wave. This stage is followed by quasi-normal ringing and the tail mode. If the scalar field has an unstable mode, we expect the effect of the instability to appear in the late time tail behavior. However, because the growth rate of the instability is very small, it may be difficult to detect the instability numerically. This is the next problem we intend to study.

Acknowledgements

We would like to thank Tomoyuki Hanawa for his suggestion regarding the numerical method used for the eigenvalue problem and Akira Tomimatsu for valuable discussions on this subject.

References

- 1) K. D. Kokkotas, *Living Rev. Rel.* **2** (1999), 2.
- 2) Y. B. Zel'dovich, *Pis'ma v Zh. Éksp. Teo. Fiz.* **12** (1970), 443.
- 3) Y. B. Zel'dovich, *Sov. Phys. JETP Lett.* **14** (1971), 180.
- 4) Y. B. Zel'dovich, *Sov. Phys. JETP* **35** (1972), 1085.
- 5) V. P. Frolov and I. D. Novikov, *Black Hole Physics* (Kluwer Academic Publishers, 1998).
- 6) W. H. Press and S. A. Teukolsky, *Nature* **238** (1972), 211.
- 7) T. Damour, N. Deruelle and R. Ruffini, *Lett. Nuovo Cim.* **15** (1976), 257.
- 8) S. Detweiler, *Phys. Rev. D* **22** (1980), 2323.
- 9) T. J. M. Zouros and D. M. Eardley, *Ann. of Phys.* **118** (1979), 139.
- 10) M. Abramowitz and I. A. Stegun, *Handbook of Mathematical Functions* (Dover, 1970).